Equilibrium configurations of 11 eV sterile neutrinos in MONDian galaxy clusters

G. W. Angus, Benoit Famaey, A. Diaferio

Monthly Notices
of the
ROYAL ASTRONOMICAL SOCIETY

Mon. Not. R. Astron. Soc. **402,** 395–408 (2010) doi:10.1111/j.1365-2966.2009.15895.x

Equilibrium configurations of 11 eV sterile neutrinos in MONDian galaxy clusters

G. W. Angus,[1,2⋆] B. Famaey[3,4] and A. Diaferio[1,2]

[1]*Dipartimento di Fisica Generale 'Amedeo Avogadro', Università degli studi di Torino, Via P. Giuria 1, I-10125 Torino, Italy*
[2]*Istituto Nazionale di Fisica Nucleare (INFN), Sezione di Torino, Torino, Italy*
[3]*AIfA, Universität Bonn, 53121 Bonn, Germany*
[4]*Observatoire Astronomique, Université de Strasbourg, CNRS UMR 7550, F-67000 Strasbourg, France*

Accepted 2009 October 15. Received 2009 October 15; in original form 2009 June 18

ABSTRACT

Modified Newtonian dynamics (MOND) can fit a broad range of galaxy kinematic data, but struggles with clusters of galaxies. MONDian clusters need dark matter (DM), and here we test the 11 eV c^{-2} sterile neutrino (SN) – used to fit the first three acoustic peaks of the cosmic microwave background (CMB) – by investigating their equilibrium distributions in 30 groups and clusters over a wide range of temperatures. We do this by first taking the known SN density, necessary for hydrostatic equilibrium of the intracluster medium (or to produce the observed lensing map). Then, we solve for the SN velocity dispersion (VD), needed for their own hydrostatic equilibrium, through the equation of state for a partially degenerate neutrino gas. The VD is a unique, continuous function of radius determined by the density and mass of the SN particles. Knowing both the SN density and VD tells us the Tremaine–Gunn phase-space limit at all radii. We find that all 30 systems serendipitously reach the Tremaine–Gunn limit by the centre, which means a portion of the dynamical mass must always be covered by the brightest cluster galaxy. Interestingly, the typical fitted K-band mass-to-light ratio is unity and at most 1.2, which is very consistent – although leaving no margin for error – with stellar population synthesis models. Amidst the sample there are several special cases including the Coma cluster (for which DM was first proposed), NGC 720 (where geometrical evidence for DM was found) and the bullet cluster (where DM – of some kind – in clusters was directly proven to exist). We demonstrate that 11 eV c^{-2} SNs are unlikely to influence spiral galaxy rotation curves, as they do not influence even some very massive early-types (NGC 4125 and NGC 6482). Finally, we conclude that it is intriguing that the minimum mass of SN particle that can match the CMB is the same as the minimum mass found here to be consistent with equilibrium configurations of MONDian clusters of galaxies.

Key words: neutrinos – dark matter – X-rays: galaxies: clusters.

1 INTRODUCTION

Sterile neutrinos (SNs) are hypothetical additions to the standard model of particle physics. They are right handed, neutral leptons that interact only via gravity, which earns them the 'sterile' prefix, contrary to the active neutrinos that also participate in the weak interaction. Gravity aside, sterile neutrinos can also interact with the active neutrinos via the quantum mechanical phenomenon of neutrino oscillations. This behaviour has been investigated by the Liquid Scintillator Neutrino Detector (Aguilar et al. 2001) and the MiniBoone experiment (Maltoni & Schwetz 2007). However, no concrete evidence was convincingly found to suggest the existence, or non-existence, of SNs from the disappearance of active neutrinos. The basis of some appeals to SNs are for aesthetic reasons, since the active neutrinos are entirely left-handed; and others make use of them in the so-called 'see-saw mechanism' which can give rise to the small masses of the active neutrinos (Lindner, Ohlsson & Seidl 2002; Kusenko 2009). More recently, Marcolli & Pierpaoli (2009) have used the framework of non-commutative geometry to develop an impressive model for the early Universe, where three SNs with Majorana mass terms emerge as a natural addition to the standard model of particle physics. Two of the SNs have masses greater than the electroweak scale (100 GeV c^{-2}) and facilitate the see-saw mechanism. The remaining SN should be light, and is strongly linked with providing the dark matter (DM) content of the Universe.

⋆E-mail: angus@ph.unito.it

Here, we make no claims of a deeper theory for SNs, but rather continue to investigate a startling coincidence identified in the recent analysis of the cosmic microwave background (CMB) by Angus (2009). There it was demonstrated that the acoustic peaks in the angular power spectrum, as measured by the *Wilkinson Microwave Anisotropy Probe* (*WMAP*; Dunkley et al. 2009) and the Arcminute Cosmology Bolometer Array Receiver (ACBAR; Reichardt et al. 2009), can convincingly be generated by a single, thermal (by virtue of neutrino oscillations in the early Universe Abazajian, Fuller & Patel 2001) SN with mass $m_{\nu_s} = 11\ \mathrm{eV\,c^{-2}}$. This SN is a straight substitution for the cold dark matter (CDM) of the concordance cosmological model (Spergel et al. 2007), such that $\Omega_{\nu_s} = 0.0205\, m_{\nu_s} = 0.225$, $\Omega_b = 0.047$ and the spectral index $n_s = 0.965$. However, whereas the unknown CDM particle can condense and form structures on virtually any scale, which puts it at odds with certain observations – like the lack of observed galactic substructure as compared to the cosmological N-body simulations (Klypin et al. 1999; Moore et al. 1999; Kroupa, Theis & Boily 2005) and the existence of DM cores in galaxy haloes (Gnedin & Zhao 2002; Gentile et al. 2004) – the hot SN free streams out of galaxies. This makes it a non-starter as a traditional DM candidate, since it would render spiral galaxies (like the Milky Way) and dwarf galaxies (like Draco and Ursa Minor) incapable of retaining their stars.

Fortunately, there is a well-studied alternative to the standard lore of gravity called modified Newtonian dynamics (MOND; see Milgrom 1983; Sanders & McGaugh 2002; Bekenstein 2006; Milgrom 2008b for reviews) which has an uncanny knack of predicting the dynamics of galaxies from a simple relation using only the baryonic matter density. The paradigm of MOND introduces a new physical constant with dimensions of acceleration, $a_o = 1.2 \times 10^{-10}\,\mathrm{ms^{-2}}$, around and below which dynamics do not follow from standard Newtonian theory. In particular, the true modulus of gravity, $g(r) = V_c(r)^2\, r^{-1}$, is not linearly related to the Newtonian gravity, $g_n(r) = GM(r)r^{-2}$, but instead

$$g = \frac{1}{2} g_n \left[1 + \sqrt{1 + \frac{4a_o}{g_n}} \right]. \quad (1)$$

This ensures adherence to two critical axioms: that gravity is Newtonian in regions of strong gravity, and that when $g_n \ll a_o$, $g \propto 1/r$ meaning rotation curves are flat at the periphery of spiral galaxies.

The additional gravity afforded by MOND, replaces the need for DM in dwarf spheroidals (Milgrom 1995; Sánchez-Salcedo & Hernandez 2007; Angus 2008; Serra, Angus & Diaferio 2009), spiral (e.g. McGaugh & de Blok 1998; Famaey & Binney 2005; Sanders & Noordermeer 2007; McGaugh 2008) and X-ray dim elliptical galaxies (Milgrom & Sanders 2003; Angus et al. 2008b) often with remarkable accuracy. It also provides the only realistic explanation of certain galaxy scaling relations – most prominently the Tully–Fisher relation (see McGaugh et al. 2000; McGaugh 2005b), but more recently the central surface brightness predicted by dark haloes (see Gentile et al. 2009; Milgrom 2009a, as well as Donato et al. 2009). Furthermore, rotation curves of tidal dwarf galaxies have been observed by Bournaud et al. (2007) and the independent analysis by Gentile et al. (2007) and Milgrom (2007) reveals not only their consistency with MOND (with zero adjusted parameters), but also constitutes a direct falsification of DM being made only of CDM in galaxies – assuming the data are reliable. What is more, Kroupa et al. (2005) have advocated that the Milky Way's dwarf spheroidal galaxies are also tidal dwarf galaxies. This convincing demonstration of MOND's predictive ability does not, however, extend to the realms of clusters of galaxies.

An obvious difference between galaxies and clusters of galaxies is simply the scale involved. If a typical galaxy is one or two tens of kpc across, clusters have accurate measurements of the gravitational potential (through the intracluster medium (ICM) or weak gravitational lensing) on scales 10 times that and therefore volumes many thousand times greater. Studies of the dynamics of groups and clusters in MOND (e.g. The & White 1988; Sanders 1994, 1999; Aguirre, Schaye & Quataert 2001; Sanders 2003; Pointecouteau & Silk 2005; Angus et al. 2007; Sanders 2007; Feix, Fedeli & Bartelmann 2008; Milgrom 2008b) have all shown that there is a huge central mass deficit and Angus, Famaey & Buote (2008a) demonstrated that active neutrinos, even at the experimental maximum ($\sim$2 $\mathrm{eV\,c^{-2}}$), cannot clump densely enough. A more plausible solution is the 11 $\mathrm{eV\,c^{-2}}$ SN proposed by Angus (2009) to fit the first three acoustic peaks of the CMB.

The feasible particle mass of SN is fully determined by fitting the CMB power spectrum, and there is virtually no freedom available above 5 per cent of the 11 $\mathrm{eV\,c^{-2}}$ mass. It is the particle mass, and particle mass alone, that sets the properties of the SNs in clusters and galaxies, although the law of gravity determines how they get there. Therefore, it is a highly intriguing corollary that the mass required to match the CMB is in the tiny range of neutrino masses (perhaps 11–12 $\mathrm{eV\,c^{-2}}$) that can both free stream out of galaxies (MOND does not require any DM in galaxies) and clump densely enough in galaxy clusters to account for the serious mass deficit exposed there.

We now have the basis of a predictive cosmological model, where we have made two positive trades. First we exchange Newtonian dynamics for MOND, which helps to explain in detail the origin of the mass discrepancy in all galaxies, and with fewer freedoms than the often contrived CDM haloes (as demonstrated by McGaugh 2005a; Kuzio de Naray, McGaugh & Mihos 2009). Secondly, we swap CDM for an 11 $\mathrm{eV\,c^{-2}}$ SN. The added bonus of SNs over CDM is that, knowing only the particle mass gives fixed predictions for the CMB and for structure formation (with a small dependence on the μ-function in only the latter case).

In the very early Universe, neutrino decoupling (both active and sterile) occurs at a temperature of $kT \sim 1\,\mathrm{MeV}$. This means that the 11 $\mathrm{eV\,c^{-2}}$ SNs (as well as the sub $\mathrm{eV\,c^{-2}}$ active neutrinos) are ultrarelativistic during decoupling, which freezes in their Fermi–Dirac distribution and their cosmological abundance is fixed (e.g. Peacock 1999). Typical CDM candidates, like 100 GeV neutralinos (e.g. Hofmann, Schwarz & Stöcker 2001) or $>100\,\mathrm{keV\,c^{-2}}$ SNs (see the review by Boyarsky, Ruchayskiy & Iakubovskyi 2009), are non-relativistic during decoupling, and self-annihilations must be used to tune the cosmological abundance. This applies to all CDM candidates which means knowing the mass of a CDM particle tells us the mass and not the cosmological abundance. Free parameters, like the interaction cross-section, must explain why they have the correct cosmological abundance.

In addition, while searching for an explanation of the anomalous low-energy excess of electron neutrinos observed by the MiniBoone experiment, Giunti & Laveder (2008) found agreement with the data by postulating a perfectly plausible renormalization of the original flux of muon-neutrinos and oscillations (that are energy dependent) from electron neutrinos to 11 ± 7 $\mathrm{eV\,c^{-2}}$ SNs. This hypothesis clearly warrants further investigation, and will be testable with the T2K neutrino experiment (Hastings 2009) which will have a near detector at $L = 280\,\mathrm{m}$ giving it a similar L/E (E being neutrino energy) as MiniBoone (M. Laveder, private communication).

In this paper, we seek to investigate the 11 eV c^{-2} SN's influence on clusters of galaxies in MOND. Primarily, we need to ascertain that every cluster has an equilibrium distribution of SNs that can account for all the missing gravitating mass. This is by no means guaranteed since there is a maximum density set by the Tremaine–Gunn limit (Tremaine & Gunn 1979, hereafter TG; see Section 3.4) depending on the velocity dispersion (VD) of neutrinos and the mass of an individual particle. If the required densities of the equilibrium models exceed the Tremaine–Gunn limit (or if the M/L of the brightest cluster galaxy (BCG) required to keep the SN density below the Tremaine–Gunn limit is too high), they would be excluded. To this end, we have taken a relatively large sample of 30 relaxed galaxy groups and clusters and have performed a straightforward procedure to gauge their consistency with the missing mass problem of clusters of galaxies in MOND.

2 DATA

We take the temperature and density profiles of the ICM in seven clusters of galaxies with temperatures in the range of 1.8–9 keV from the sample of Vikhlinin et al. (2006), a further 13 groups of galaxies from the sample of Gastaldello et al. (2007), the cluster A 2589 from Zappacosta et al. (2006) and three X-ray bright, isolated early-type galaxies from the sample of Humphrey et al. (2006). This covers the full sample used in Angus et al. (2008a), but in addition, we make an analysis of the two clusters comprising the bullet cluster (Clowe, Gonzalez & Markevitch 2004; Bradač et al. 2006; Clowe et al. 2006; Angus et al. 2007) working from the Navarro–Frenk–White (NFW) haloes fitted to the weak-lensing convergence map. We also take a fitted NFW profile for the cluster A 1689 from the strong lensing analysis of Halkola, Seitz & Pannella (2006), take three estimates for the density profile of the Coma cluster (Gavazzi et al. 2009; Kubo et al. 2007), a pair of clusters in the Lynx field (Jee et al. 2006) and the fossil group RXJ 1416 (Khosroshahi et al. 2006).

For the Gastaldello et al. (2007) sample, we only had X-ray data for 10 of the 13, so for the other three (A 2717, IC 1860, MS 1160), we started from their fitted NFW (Navarro, Frenk & White 1997) profiles and included the BCG.

In Vikhlinin et al. (2006), the authors give fully analytical descriptions of the ICM temperature and density allowing us to solve the equation of hydrostatic equilibrium to give the dynamical mass of each cluster (see Section 3). Similarly, for the groups of galaxies, we were provided with (D. Buote, private communication) high-resolution data that gives the ICM density and temperature as functions of radius. We fitted β-models to the ICM density and have fitted the same analytical models defined in Vikhlinin et al. (2006) to the temperature. These models are rather sophisticated, many parameter models that maximize the accuracy of the fits.

The masses of the BCGs are taken either from the Gastaldello et al. (2007), Vikhlinin et al. (2006), Humphrey et al. (2006) and Zappacosta et al. (2006) K-band luminosity estimates, the observations of Lin & Mohr (2004) or from K-band magnitudes on the NASA/IPAC Extragalactic Database (NED) data base as per Angus et al. (2008a).

Naturally, there are errors associated with the best-fitting density and temperature profiles, which we do not explicitly investigate here. It is enough to say that the observational uncertainties surrounding the Newtonian dynamical mass (from which everything is deduced) are no larger than the uncertainties in the triaxiality of the cluster or the interpolating function used to find the MONDian dynamical mass, so we waste little time debating them. Moreover, we use a sample containing 30 of some of the most relaxed systems so that a general consensus can be reached, and problematic systems or special cases are discussed in Section 4.1.

3 SOLVING FOR SN EQUILIBRIUM CONFIGURATIONS

3.1 Intracluster medium hydrostatic equilibrium

The density of 11 eV c^{-2} SNs (or any DM candidate) in MONDian clusters of galaxies required to sustain hydrostatic equilibrium of the ICM is given by the following steps, as per Angus et al. (2008a). First, we take the observed density and temperature of the ICM, $\rho_x(r)$ and $kT_x(r)$, respectively, and numerically take their logarithmic derivative with respect to radius to find the true gravity as a function of radius:

$$g(r) = \frac{-kT_x(r)}{wm_p r}\left[\frac{\mathrm{d}\ln\rho_x(r)}{\mathrm{d}\ln r} + \frac{\mathrm{d}\ln kT_x(r)}{\mathrm{d}\ln r}\right], \tag{2}$$

where $w = 0.62$ is the mean molecular weight of the ICM. The gravity is directly related to the total MOND enclosed mass by

$$M_\mathrm{m}(r) = r^2 G^{-1} g(r)\mu(g/a_\mathrm{o}), \tag{3}$$

and the interpolating function is the simple one:

$$\mu(g/a_\mathrm{o}) = \frac{g/a_\mathrm{o}}{1 + g/a_\mathrm{o}} \tag{4}$$

(see Famaey et al. 2007 for a discussion of how it fares in spirals). This single line is the only stage at which MOND is involved.

After subtracting the mass of the ICM [$M_x(r) = \int_0^r 4\pi\hat{r}^2\rho_x(\hat{r})\mathrm{d}\hat{r}$], we are left with the SN mass distribution and the unsubtracted BCG, $M_\mathrm{bcg} + M_{\nu_\mathrm{s}}(r) = M_\mathrm{m}(r) - 1.15M_x(r)$, where the mass of the BCG is $M_\mathrm{bcg} = M/L_K \times L_{K,\mathrm{bcg}}$. The 1.15, which is of virtually no consequence (we tried 1.5 with no difference), multiplies the ICM mass to include the contribution of galaxies in the cluster. We invert this to give the SN density

$$\rho_{\nu_\mathrm{s}}(r) = (4\pi r^2)^{-1}\frac{\mathrm{d}}{\mathrm{d}r}M_{\nu_\mathrm{s}}(r). \tag{5}$$

Although it is vitally important, we ignore the BCG until later for reasons that will become obvious.

3.2 Sterile neutrino hydrostatic equilibrium

At this point, we have a deduced density of SNs in a cluster of given temperature profile: at least it is the density exactly required for hydrostatic equilibrium of the ICM (or in the case of lensing, to create the observed convergence map). In addition to this constraint, there is an equation for hydrostatic equilibrium of the SNs themselves, which is crucial to this analysis. This invokes the equation of state of neutrinos (active or sterile; see e.g. Sanders 2007) and what this gives us are equations that define the density and pressure of a partially degenerate neutrino gas, coupled via the hydrostatic equilibrium relation:

$$\frac{\mathrm{d}}{\mathrm{d}r}P_{\nu_\mathrm{s}} = -\rho_{\nu_\mathrm{s}}(r)g(r). \tag{6}$$

To express the density, we start with the equilibrium occupation number

$$f = \frac{1}{\exp(x - \chi) + 1}, \tag{7}$$

where x and χ are, respectively, the ratios of neutrino energy and chemical potential to temperature. A large positive or negative χ

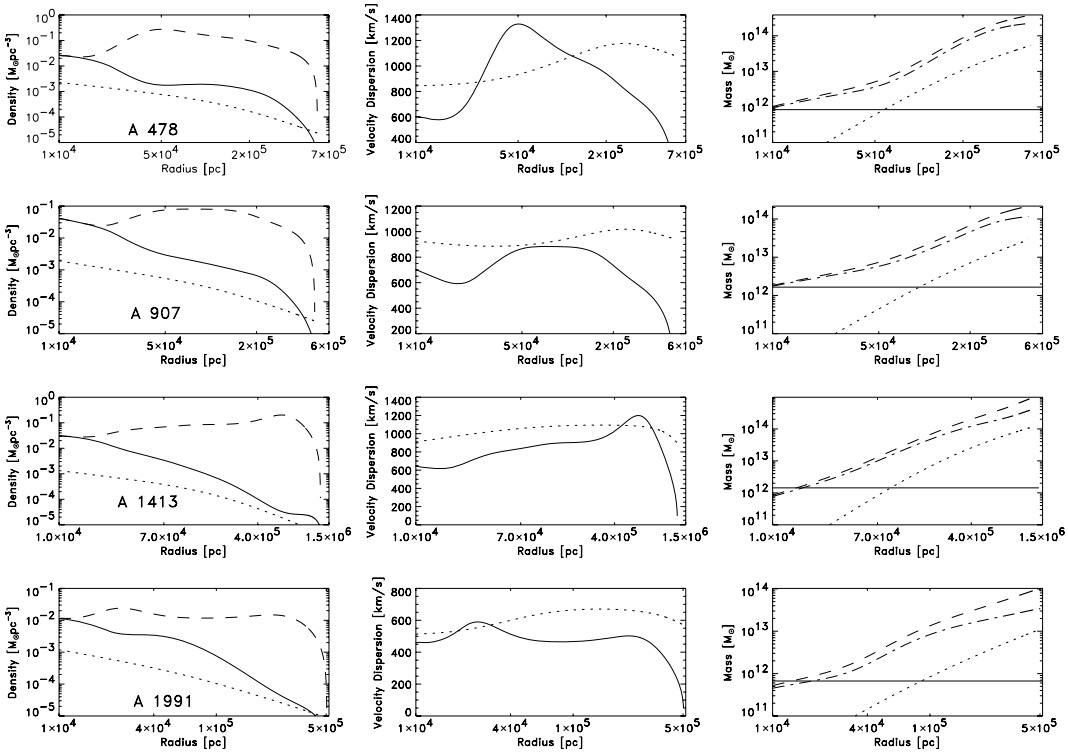

Figure 1. As per Figs 2–6, each row refers to a specific cluster, whereas the columns are properties of that cluster. In the left-hand panels, we plot density against radius for SNs (solid), ICM (dotted) and Tremaine–Gunn limit (dashed). In the central panels, we plot VD against radius for SNs (solid) and ICM (dotted). In the right-hand panels, we plot enclosed mass against radius for the Newtonian dynamical mass (dashed), MOND dynamical mass (dot–dashed), ICM (dotted) and the total mass of the BCG (solid). Each cluster's designation is inscribed on the left-hand panel.

denotes strong degeneracy or non-degeneracy, respectively. From this we find the phase-space density

$$n = g_\nu h^{-3} m_{\nu_s}^4 f. \tag{8}$$

Here, $h = 4.136 \times 10^{-15}$ eV s is Planck's constant and $g_{\nu_s} = 2$ takes into account the antiparticles, whilst remembering that neutrinos have only a solitary helicity state. One immediately sees that there is an absolute upper limit to the allowed density of SNs in phase space, corresponding to full degeneracy ($\chi = +\infty$, $f = 1$) and known as the Pauli limit. However, the starting momentum distribution of neutrinos in the early universe corresponds to half this limit ($\chi = 0$, $f = \frac{1}{2}$).

In groups and clusters of galaxies, SNs with a rest mass of 11 eV c^{-2} are non-relativistic since they are travelling at velocities of the order of 100–1000 km s^{-1} (e.g. Fig. 1, central panels), therefore, neutrino energy is simply related to momentum by $E = p^2/2m_{\nu_s}$. The number density of neutrinos is given by $\int f d^3p$ and multiplying this by SN mass ($m_{\nu_s} = 11$ eV c^{-2}), converting momentum to energy and temperature to VD ($kT_{\nu_s} = m_{\nu_s}\sigma_{\nu_s}^2$) we find our equation for neutrino mass density:

$$\rho_{\nu_s}(r) = 4\sqrt{2}\pi g_\nu h^{-3} m_{\nu_s}^4 \sigma_{\nu_s}^3(r) F_{1/2}(\chi), \tag{9}$$

where the SN VD and temperature are σ_{ν_s} and kT_{ν_s}, respectively, and $F_{1/2}(\chi) = \int_0^\infty x^{1/2} f(\chi)\,\mathrm{d}x$. In a non-relativistic neutrino gas, the pressure is equal to 2/3 the internal energy per unit volume ($U_{\nu_s} = \int E(p) f d^3p$) giving

$$P_{\nu_s}(r) = \frac{8\sqrt{2}\pi}{3} g_\nu h^{-3} m_{\nu_s}^4 \sigma_{\nu_s}^5(r) F_{3/2}(\chi), \tag{10}$$

where

$$F_{3/2}(\chi) = \int_0^\infty x^{3/2} f(\chi)\,\mathrm{d}x.$$

It emerges that there are two variables here that must be set in order for the neutrinos to exist in hydrostatic equilibrium. Primarily, $\chi(r)$ must be set so that the fixed density of equation (5) is matched by equation (9). In case this is not obvious, we solve equation (9) for $F_{1/2}(\chi)$, for which there is a unique, continuous $\chi(r)$ once the neutrino VD is given. There is no independent method, apart from cosmological simulations of the collapse of the baryonic plus SN two-fluid mixture to estimate the chemical potential, χ, so we choose here to fit it to the data. Whether detailed numerical simulations of cluster formation in a MOND cosmology will reproduce this chemical potential will be a crucial test of the equilibrium models presented hereafter.

This $\chi(r)$ is then transferred to equation (10), and although $\chi(r)$ is used to balance $\rho_\nu(r)$ and ensure it remains unchanged when σ_{ν_s} is varied, it influences the pressure, P_{ν_s}, non-linearly. Secondly, equation (6) must be satisfied, however, it is not satisfied if we make the assumption that the SN VD is identical to the ICM VD. In general, there would be too much pressure because the neutrinos would be too hot for their given distribution.

A priori, there is no reason that the 11 eV c^{-2} SNs should have precisely the same temperature as the ICM. Both fluids are orbiting in the same gravitational potential, but there is no rapid exchange mechanism to bring them into mutual equilibrium, as there was in the very early Universe. In fact, this is likely to be related to the formation epoch of the cluster, where the SN haloes would have

formed at relatively high redshift while the Universe was more dense. Later, the ICM would have fallen into the deep potential well, created by the SN halo, and therefore it is logical that the ICM should be hotter than the SNs.

In addition to probing the $\chi(r)$'s fitted, numerical simulations of galaxy clusters in MOND will, in time, be able to tell us if the differences between the SN and ICM VDs are realistic.

From equations (9) and (10) one can see that the SN VD influences the product of the density and gravity (the right-hand side of equation 6) non-linearly with respect to the gradient of the neutrino pressure. Essentially, to force the SN distribution into hydrostatic equilibrium, with its fixed density, we can modify the SN VD. However, as we shall discover in the next section, this cannot be achieved by a simple scaling from the ICM VD, but instead by solving for the neutrino VD, σ_{ν_s}, as a unique, continuous function at every radius.

3.3 Solving for a unique SN velocity dispersion

In principle, for hydrostatic equilibrium of the SNs, we need $\frac{\frac{\mathrm{d}}{\mathrm{d}r}P_{\nu_s}(r)}{\rho_{\nu_s}(r)g(r)} = -1$ and inserting equations (9) and (10) gives us

$$\sigma_{\nu_s}(r)\frac{\mathrm{d}}{\mathrm{d}r}\sigma_{\nu_s}(r) + \frac{\sigma^2_{\nu_s}(r)}{5F_{3/2}(r)\frac{\mathrm{d}}{\mathrm{d}r}F_{3/2}(r)} = -\frac{3}{10}\frac{F_{1/2}(r)}{F_{3/2}(r)}g(r). \quad (11)$$

Using the substitution $\epsilon(r) = \sigma^2_{\nu_s}(r)$, leading to $\epsilon'(r) = 2\sigma_{\nu_s}(r)\sigma'_{\nu_s}(r)$ and the integrating factor $F_{3/2}(r)^{0.4}$, we can reduce this first order linear differential equation to

$$\sigma^2_{\nu_s}(r) = \frac{3}{5}F_{3/2}(r)^{-0.4}\int_{\infty}^{r}\frac{F_{1/2}(\hat{r})}{F_{3/2}(\hat{r})^{0.6}}g(\hat{r})\mathrm{d}\hat{r}. \quad (12)$$

To find pressure and density in the first instance, we must submit a trial σ_{ν_s} to equation (12): typically we try $\frac{1}{2}\sigma_x$, where the ICM VD is defined by

$$\sigma_x = c \times \left(\frac{kT_x}{wm_\mathrm{p}}\right)^{1/2}. \quad (13)$$

Here, $c = 3 \times 10^5\,\mathrm{km\,s^{-1}}$ is the speed of light, kT_x is the ICM temperature in keV, $w = 0.62$ is again the mean molecular weight and $m_\mathrm{p} = 9.38 \times 10^5\,\mathrm{keV}$ is the mass energy of a proton. From the trial solution, we iterate rapidly towards convergence. The final $\sigma_{\nu_s}(r)$ gives hydrostatic equilibrium to better than 1 per cent at all radii and most importantly is unique – set only by the SN mass and its deduced density from equation (5).

3.4 Phase-space constraints

We now have a unique correlation between the density of SNs and their VDs. This is important because these two variables define the phase-space distribution of the SNs, to which there is a fundamental limit.

Liouville's theorem states that (in the absence of encounters) flow in phase space is incompressible and that each element of phase-space density is conserved along the flow lines. However, this only applies to the fine-grained phase-space density of an infinitesimal region. Rather, for the observable, which is the coarse-grained (macroscopic) phase-space density, we simply must not exceed the maximum of the fine-grained one.

Thus, the SN phase-space density must not increase during collapse, from its starting value of $\frac{1}{2}g_\nu h^{-3}m^4_{\nu_s}$ (which is half the Pauli degeneracy limit) to its current maximum value of $\rho_{\nu_s}(r)[2\pi\sigma^2_{\nu_s}(r)]^{-1.5}$ (where we assume the velocity distribution is locally Gaussian everywhere with dispersion σ_{ν_s}). This limit is called the Tremaine–Gunn limit (TG) and rearranging it in terms of the critical density for an 11 $\mathrm{eV\,c^{-2}}$ SN, where $1\,\mathrm{eV\,c^{-2}} = 8.9 \times 10^{-67}\,\mathrm{M_\odot}$ and $s^3c^3 = 9.18 \times 10^{-25}\,\mathrm{pc^3}$ (where s is obviously 1 s) gives us

$$\rho_{\nu_s,\mathrm{TG}}(r) = 3.15 \times 10^6\left[\frac{\sigma_{\nu_s}(r)}{c}\right]^3\,\mathrm{M_\odot\,pc^{-3}}. \quad (14)$$

The important thing to bear in mind here is that this is a significantly more accurate estimate of the TG limit because it is calculated from the unique, derived SN VD exactly necessary for hydrostatic equilibrium and not by assuming some relation between the ICM and the neutrinos, as is often the case (Angus, Famaey & Buote 2008a; Gentile, Zhao & Famaey 2008; Natarajan & Zhao 2008). Therefore, we have the TG limit as a function of radius, since we know the derived value of the VD from solving equation (12).

Let us note however that departures from Gaussianity in the velocity distribution could perhaps somewhat affect this physical upper limit on the SN density, as well as non-isotropy of the SN velocity distribution, or triaxiality of the SN halo.

The consequence of the TG limit is that if the density of SNs required for cohesion of the cluster gas exceeds the TG limit (in particular at the centre), then the MOND plus 11 $\mathrm{eV\,c^{-2}}$ SN hypothesis would be ruled out.

4 RESULTS

In Figs 1–6, we present the densities, VDs and enclosed mass profiles for the 30 groups and clusters. In the left-hand panels, we plot the SN density (solid line type), ICM density (dotted) and the TG limit of the cluster (dashed) against radius. In the middle panels, we plot both the observed ICM (dotted) and the derived (from equation 12) SN (solid) VD as functions of radius. In the right-hand panels, we plot each cluster's enclosed Newtonian dynamical mass (dashed), MOND dynamical mass (dot–dashed), BCG total mass with unity M/L (solid) and ICM mass (dotted).

There are a few salient features to observe: primarily, the SN VD (or temperature) is in most cases 20–50 per cent lower than the ICM VD. The simple explanation, alluded to earlier, is that the SN haloes presumably formed at relatively high redshift, through only their mutual gravitation. On the other hand, the ICM fell from large distances, through the already present, deep potential well of the SNs and thus had greater potential energy to transfer to kinetic energy, although this still has to be demonstrated with numerical simulations.

Taking a closer look at the SN densities and VDs, they have conspicuous kinks around 20–30 kpc. This radius, r_tg, is where the density reaches the TG limit. If no phase-space limit existed, the SN density would continue to increase towards the Pauli limit and the neutrino equation of state would begin to substantially change from non-degeneracy (large negative χ) $P_{\nu_s} \propto \rho_{\nu_s}\sigma^2_{\nu_s}$ to the degenerate one (large positive χ) $P_{\nu_s} \propto \rho^{5/3}_{\nu_s}$ [where χ of the TG limit is numerically identified with 0.35 instead of zero because equation (14) assumes a Gaussian distribution].

However, since we must adhere to the TG limit, we impose it by making the density equal to the TG limit at all radii smaller than r_tg. The density and VD both increase towards the centre as they must conform to the dual constraints of remaining at the TG limit and satisfying hydrostatic equilibrium. Alternatively, if we had ignored the TG limit, the VD would have crashed towards the centre of the cluster; as less classical pressure would be required to prop up the SN halo. This is simply because gradually more Fermi pressure would be available. It is this behaviour that causes the kink since

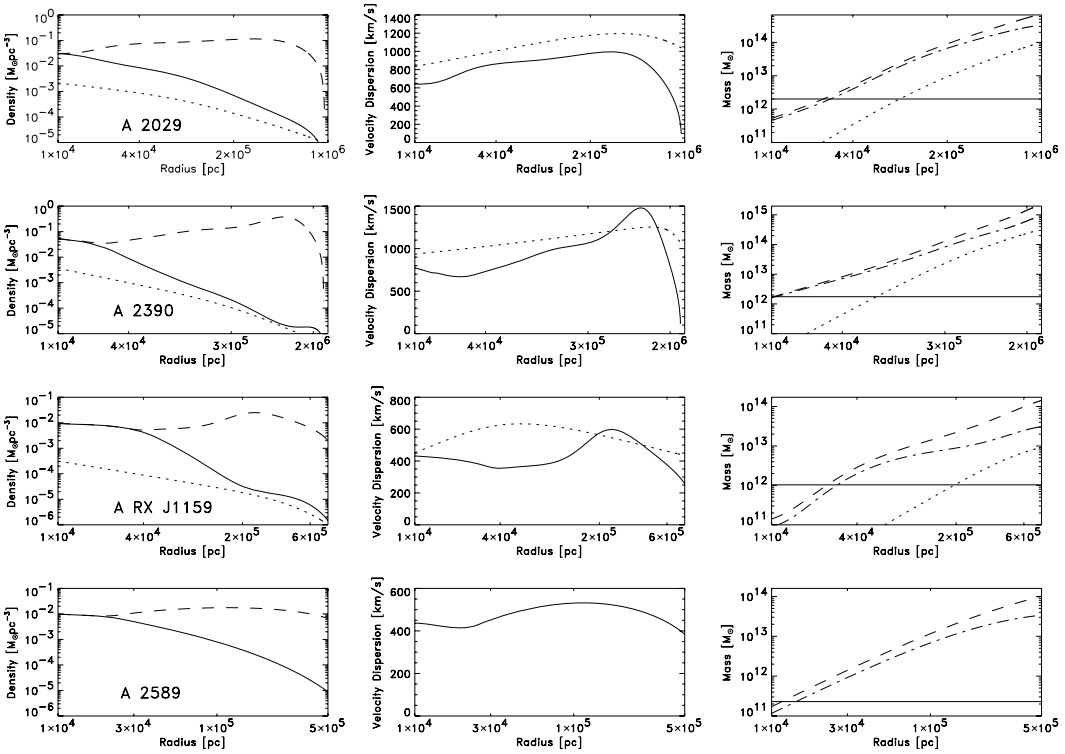

Figure 2. As per Fig. 1.

we force the density to be equal to the TG limit, the VD required for hydrostatic equilibrium must rise, whereas it was falling prior to this.

Since the SN halo of every group and cluster reaches the TG limit at $r_{\rm tg}$ when there is still a discrepancy between the central SN density and the required total density for hydrostatic equilibrium of the gas, the BCG plays a crucial role in determining how satisfactory our 11 eV c^{-2} SN hypothesis is. If no BCG existed in any of our clusters, they would immediately fail.

We know the luminosity of most BCGs in the K-band which gives an excellent indication of mass (see e.g. Bell & de Jong 2001; Humphrey et al. 2006; Gastaldello et al. 2007; Conroy, Gunn & White 2009) and we know a few in other bands (B, V, R) or not at all. Therefore, we must modify the M/L_K (given in Table 1) to exactly match $M_{\rm m}$ at $r_{\rm tg}$, which basically means the BCG is picking up all the excess left when the SN reaches the TG limit and can no longer account for the full dynamical mass.

There are some points to bear in mind, first the highest M/L_K used was 1.2 and the lowest 0.1. In the latter case, of a very low M/L_K, this can be due to the total luminosity not being enclosed by $r_{\rm tg}$ (which can be as low as 10 kpc, but usually ∼20–30 kpc). In the case of $M/L_K \sim 1$, this can be considered a fitting parameter, since there is no freedom in the cluster to have a M/L_K lower than the value used because the SN density reaches the TG limit at the centre of every cluster. Furthermore, the M/L_K cannot be significantly larger or it would be in disagreement with the typical M/L_K demonstrated by Bell & de Jong (2001). In the cases, where $M/L_K < 0.8$, it need not be considered a fitting parameter, since there is freedom for the M/L_K to be larger and simply for the SN density to be lower. Nevertheless, the TG limit will still be reached in every cluster, the only difference will be that if we are underestimating the BCG mass then $r_{\rm tg}$ will simply be lower for that particular cluster. The only reason we fix the density to be equal to the TG limit for all radii smaller than $r_{\rm tg}$ is to highlight the maximum amount of luminosity the BCG could lose (e.g. if observations are incorrect) and still provide the required central density profile.

Generally, it is interesting to note that the SN haloes needed to fit galaxy clusters here have a density slope similar to that of the ICM in the central parts, but becoming sharper at intermediate distance, which is accompanied by a relatively flat VD. At the edges of the clusters, the ICM density becomes larger than the SN density (which falls to zero) and there is an apparent sharp decrease of the SN VD to zero also. This is merely a numerical artefact of the SN density being set to zero at the edges of clusters, under the assumption of hydrostatic equilibrium. Since the SN density will in reality fall to a very small number, but still greater than zero, the VD will actually be isothermal, as we would expect.

4.1 Individual systems

Below we discuss some pertinent observations about individual groups or clusters.

4.1.1 The bullet cluster

Analysis of the CMB strongly favours the hypothesis that non-baryonic DM exists in the Universe, and the bullet cluster (Clowe et al. 2006) compounds it (although Milgrom 2008a has suggested that the DM of clusters could be ultra cold and collisionless clumps of molecular gas which would satisfy the constraint of this particular cluster). As two giant galaxy clusters crashed into each other at incredible speed (Markevitch et al. 2002, but see also Angus & McGaugh 2008 for why this might pose a problem for Λ CDM),

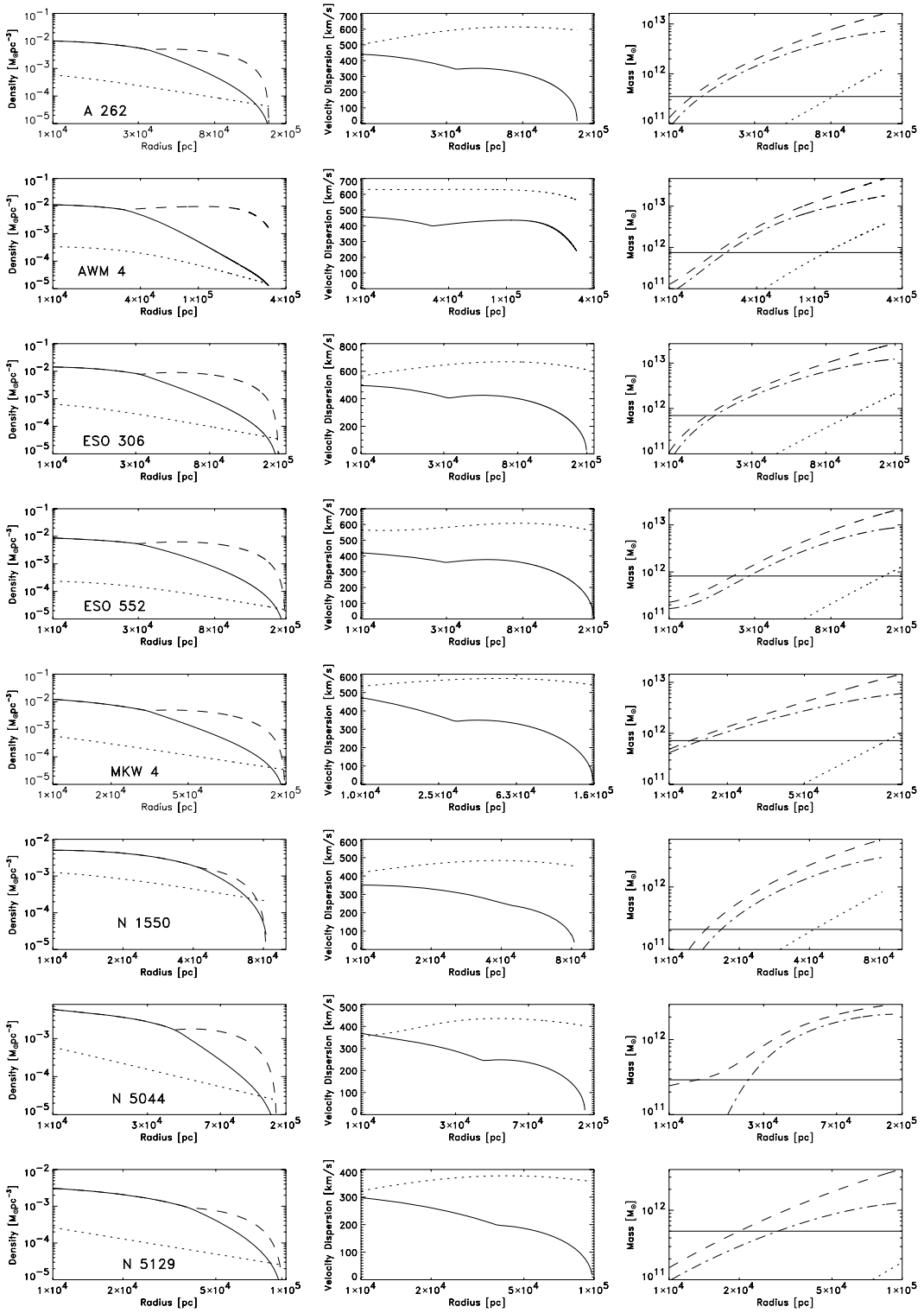

Figure 3. As per Fig. 1.

mutual ram pressure from the two ICMs caused them to decelerate, and separated them from the galaxies and the DM, which passed through and emerged on the opposite sides on the sky. A weak-lensing reconstruction required two DM haloes to overlay the positions of the galaxies with NFW parameters for the main and subcluster, respectively – $M_{200} = 15.0, 1.5 \times 10^{14}\,\mathrm{M}_{\odot}$, $r_{200} = 2.1$, 1.0 Mpc and concentrations $c = 1.94, 7.12$.

In this case, where we are directly given the Newtonian mass profile, we begin the procedure at equation (3) and follow the same steps. As with the other clusters, in Fig. 6, we show that the SN haloes in these two clusters both reach the TG limit smoothly at the centre. However, note we must add a $3.5 \times 10^{11}\,\mathrm{M}_{\odot}$ stellar mass to the subcluster (labelled 'Bullet 2') to cover the dynamical mass in the central 30 kpc, which is very significant. The stellar

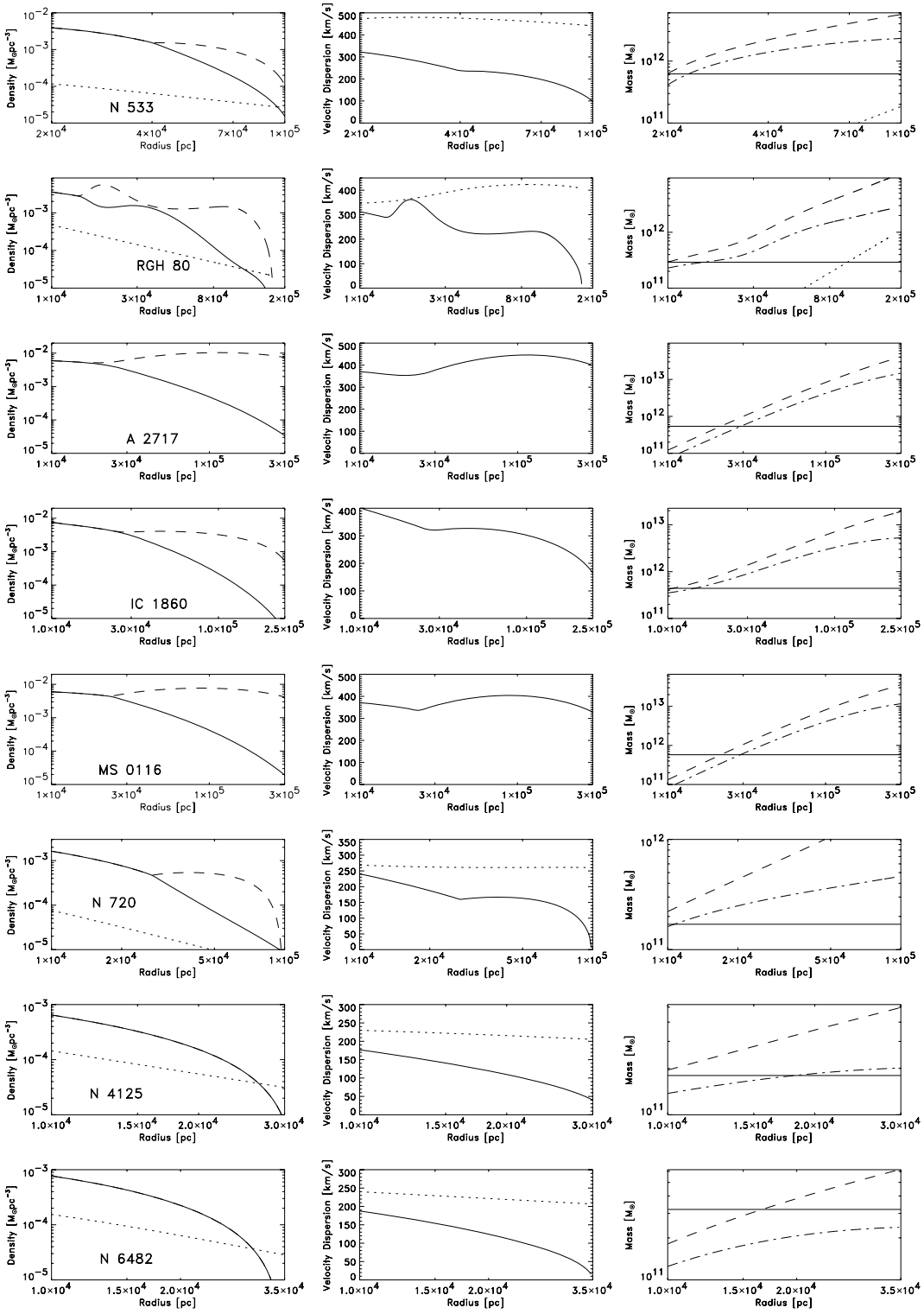

Figure 4. As per Fig. 1, except that certain lines corresponding to the ICM are absent because the SN densities were deduced from weak or strong lensing analyses.

mass quoted in Clowe et al. (2006) at the weak-lensing peak of the subcluster is $(5.8 \pm 0.9) \times 10^{11}\,\mathrm{M}_{\odot}$ within 100 kpc, from I-band observations assuming a M/L_I of 2. We need only add a trivial stellar mass of $10^{11}\,\mathrm{M}_{\odot}$ to the main cluster, which is interesting since one can see from the left-hand panel of Fig. 1 from Clowe et al. (2006) that there is no obvious BCG candidate associated with it. In fact, the two giant ellipticals of the main cluster highlighted by Clowe et al. (2006) are roughly 50 kpc (to the northern one) and 75 kpc (to the eastern one) from the lensing peak, but can easily offer the necessary stellar mass. On the other hand, the centre of the BCG of the subcluster is only roughly 25 kpc from the lensing peak and considerable light is spilling over within 10 kpc. Furthermore,

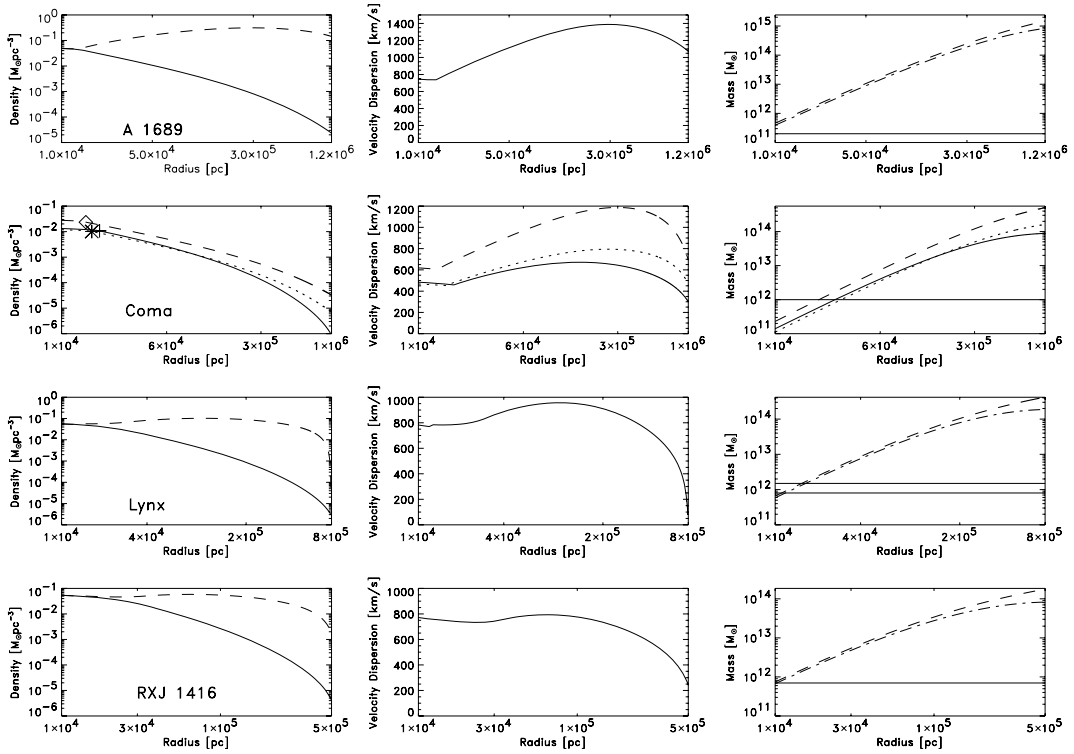

Figure 5. As per Figs 1–4, except that they are for A 1689 (Halkola et al. 2006), the Coma cluster, the two clusters that comprise the Lynx cluster (Jee et al. 2006) and the fossil group RXJ 1416 (Khosroshahi et al. 2006), from which the masses are taken in NFW form. For the Coma cluster, we use three different measurements for the NFW mass profile as discussed in detail in Section 4.1.1. To avoid crowding the Coma density plot, we only plot the SN density for NFW profile 1 (solid), 2 (dotted) and 3 (dashed) and not the Tremaine–Gunn limit, which is instead marked by an asterisk, plus sign and diamond, respectively, where the SN density reaches it.

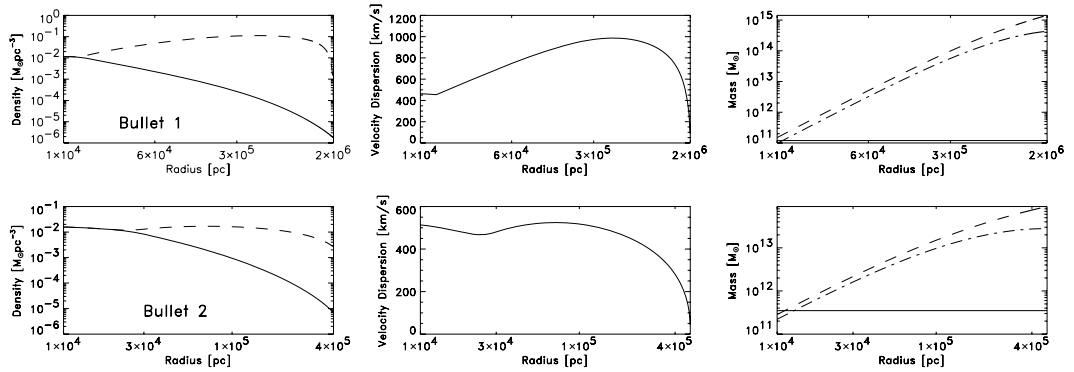

Figure 6. As per Figs 1–5, except that they are for the two clusters that comprise the bullet cluster (Clowe et al. 2006), from which the masses of the two clusters are taken in NFW form. This case is discussed in detail in Section 4.1.1.

since BCGs usually dominate the stellar mass in the central 100 kpc of clusters, the majority of the $5.8 \pm 0.9 \times 10^{11}\,\mathrm{M}_{\odot}$ is likely associated with it, making the $3.5 \times 10^{11}\,\mathrm{M}_{\odot}$ plausible. Note also that the $3.5 \times 10^{11}\,\mathrm{M}_{\odot}$ is not required within 10 kpc, but rather by 30 kpc. Within 10 kpc less than $1.5 \times 10^{11}\,\mathrm{M}_{\odot}$ is required.

4.1.2 RGH 80

Another intriguing point about BCG masses is the one used for the group RGH 80, which has two equally massive central galaxies: NGC 5098a and NGC 5098b with $L_K = 2.9 \times 10^{11}\,\mathrm{L}_{\odot}$ and $2.4 \times 10^{11}\,\mathrm{L}_{\odot}$, respectively. In our previous paper (Angus et al. 2008a), we were only interested in the central 100 kpc, therefore, were able to combine the two galaxy luminosities together. However, only one of the galaxies is at the very centre (see fig. 9 of Mahdavi et al. 2005 or fig. 1 of Randall et al. 2009), and the other has a projected separation of around 50 kpc and possibly a considerable line-of-sight distance. Before removing the second galaxy, the TG limit was considerably larger than the maximum central density, but after discounting it, the TG limit is reached at 20 kpc.

4.1.3 Clusters with no BCG luminosity: A 1689 and A 2390

We found no galaxy luminosities for the two clusters A 1689 and A 2390, but they require BCGs with total masses of at least 2.0 and $18.5 \times 10^{11}\,\mathrm{M}_{\odot}$, respectively, which is a prediction of this model.

Table 1. List of the K-band luminosities of our BCGs along with the minimum K-band mass-to-light ratio required to fit the dynamical mass.

Cluster	L_K ($10^{11}\,L_\odot$)	Min M/L_K
A 262	4.1	1.0
AWM 4	7.5	0.3
ESO 306	7.0	1.0
ESO 552	8.2	0.3
MKW 4	7.2	1.1
NGC 1550	2.1	1.2
NGC 5044	2.9	1.1
NGC 5129	5.0	0.6
NGC 533	1.2	1.0
RGH 80	2.9	0.8
A 478	8.4	1.2
A 907	16.5	1.1
A 1413	18.3	0.4
A 1991	6.9	0.65
A 2029	20.1	0.2
A 2390	18.5*	...
RXJ 1159	10.3	0.4
NGC 720	1.7	1.2
NGC 4125	1.8	0.9
NGC 6482	3.2	1.0
A 2589	2.3 (V)	0.65
A 2717	5.4	0.2
IC 1860	4.4	1.0
MS 0116	5.8	0.25
A 1689	2.0*	...
Coma	$\sim$10.0	0.15/0.1/0.2
Lynx	15, 8 (B)	0.4, 0.75
RXJ 1416	7.0 (R)	1.2
Bullet 1	1.0*	...
Bullet 2	3.5*	...

Note. The clusters with a (*) lack information about the BCG, so in the luminosity column, we have entered the required BCG luminosity with unity M/L. The clusters with a luminosity followed by (V), (B) or (R) have their luminosity measured in that band, and not the K-band. The Coma cluster has three separate mass profiles, so the 3 M/Ls refer to the profiles in the order they are taken in Fig. 5. The clusters are separated into samples: the top set are from the Gastaldello et al. (2007) sample; then the Vikhlinin et al. (2006) sample; Humphrey et al. (2006); Zappacosta et al. (2006); miscellaneous NFW fits; the bullet cluster.

Interestingly, A 1689 has been used extensively to argue against CDM by Broadhurst & Barkana (2008) because the observed NFW concentration parameter is considerably larger than that expected from cosmological simulations. We find the equilibrium model with 11 eV c^{-2} SNs nicely reaches the TG limit at 20 kpc, even though it has one of the highest central SN densities of all our sample.

4.1.4 Lynx

The two clusters in the Lynx field are in the process of merging (like the bullet cluster) and thus the mass profiles are potentially overlapping. Nevertheless, their offset seems to be sufficiently large to get a reasonable estimate from weak lensing and this has also been sanity checked with X-ray hydrodynamics (Jee et al. 2006). Both the larger cluster and smaller cluster are fitted with the same NFW profile: $M_{200} = 2.0 \times 10^{14}\,M_\odot$, $r_{200} = 0.75$ Mpc and concentration $c = 4$. The galaxy luminosities within 500 kpc of each of the two lensing peaks are 15 and $8 \times 10^{11}\,L_\odot$ in the B-band. We require $6.0 \times 10^{11}\,M_\odot$ for each BCG, which is easily affordable by the luminosity of both clusters because typical B-band M/Ls can range between 1 and 4.

4.1.5 Coma

The historical importance of the Coma cluster with respect to the DM problem is probably far more significant than its scientific merit in this present case, but we include it out of curiosity. It was originally analysed in MOND by The & White (1988) and was actually concluded to be more or less consistent with MOND – although the galaxies required radially biased orbits and the acceleration constant, a_o, had to be increased by at least a factor of 2 from the one used here. The problem with Coma is that it is not particularly relaxed and also its sphericity is questionable. For example, Neumann et al. (2003) showed that there is ongoing merging, which makes measurements of the central mass profile uncertain. Therefore, the only way to get a decent estimate of the dark halo of Coma is to use weak lensing (like we have done with the bullet cluster), but even then the assumption of spherical symmetry is dubious. The best study of Coma was performed by Gavazzi et al. (2009), but unfortunately they found only a rather speculative NFW profile of $M_{200} = 5.1^{+4.3}_{-2.1} \times 10^{14}\,M_\odot$ and $r_{200} = 1.8^{+0.6}_{-0.3}$ Mpc with no prior on the concentration parameter (found to be $c_{200} = 5.0^{+3.2}_{-2.5}$). With a prior on the concentration parameter (set to be $c_{200} = 3.5^{+1.1}_{-0.9}$), they found $M_{200} = 9.7^{+6.1}_{-3.5} \times 10^{14}\,M_\odot$ and $r_{200} = 2.2^{+0.3}_{-0.2}$ Mpc. Finally, we added an estimate from Kubo et al. (2007): $M_{200} = 27.0 \pm 8.0 \times 10^{14}\,M_\odot$, $r_{200} = 2.9 \pm 0.3$ Mpc and $c_{200} = 3.8^{+13.2}_{-1.8}$. The mass of the central galaxy would need to be 1.5, 1.0 and $2.0 \times 10^{11}\,M_\odot$, respectively, for the three cases. The K-band luminosity of the central galaxy in Coma is $10^{12}\,L_\odot$, so there is sufficient galactic mass to supply what is needed.

4.1.6 RXJ 1416

We included one fossil group RXJ 1416 in the sample since it has a very minor galaxy component (aside from the BCG). Khosroshahi et al. (2006) fitted an NFW profile to X-ray data from *Chandra* and *XMM–Newton* with parameters $M_{200} = 3.1 \times 10^{14}\,M_\odot$, $r_{200} = 1.2$ Mpc and $c_{200} = 11.2 \pm 4.5$ and we used it to infer the necessary M/L of the BCG which has luminosity $L_R = 7 \times 10^{11}\,L_\odot$. The M/L_R need only be 1.2, whereas 5 is a typical value for an old stellar population in that band. So here again, as with several of the other massive systems, the full luminosity of the BCG is not required, although the SN halo reaches the TG limit at the centre. This might be because the BCG is extended and only a fraction of the light is enclosed within 20 or 30 kpc (where the SN halo reaches the TG limit). Alternatively, if we used the full mass of the BCG, the SN density would simply reach the TG limit at a smaller radius.

4.1.7 NGC 4125 and NGC 6482

These two X-ray bright early-type galaxies were taken from the sample of Humphrey et al. (2006). Interestingly, from the point of view of SNs in galaxies (which could disrupt the good fits to rotation curves, i.e. the basis of MOND), their dynamical masses are comfortably covered by the BCG mass everywhere. From their density figures you can see the SNs are at the TG limit everywhere, but the SNs make virtually no impact on their mass profiles. In fact,

if the SN density for NGC 4125 was $8 \times 10^{-4}\,\mathrm{M}_\odot\,\mathrm{pc}^{-3}$ all the way to the centre from 10 kpc, the enclosed mass of SNs would be $3.4 \times 10^9\,\mathrm{M}_\odot$ in comparison to roughly $1.0 \times 10^{11}\,\mathrm{M}_\odot$ for the BCG (at that radius), which is a factor of 30. Therefore, there is no reason to believe that SNs will influence the internal dynamics of individual galaxies in a meaningful way.

4.1.8 NGC 720 and NGC 1550

These are the two most problematic groups. Buote & Canizares (1994, 1996) and Buote et al. (2002) observed that the twisting of X-ray isophotes around the elliptical galaxy NGC 720 compared to the intrinsic ellipticity of the galaxy (which outweighs the gas by more than two orders of magnitude) could only be compatible with the presence of DM at least four times the galaxy mass (by the edge of the galaxy). This SN halo would have an ellipticity distinct to that of the galaxy and the gas would trace the superimposed potential, hence generating the twisting isophotes. The luminosity of NGC 720 is $L_K = 1.7 \times 10^{11}\,\mathrm{L}_\odot$ and requires $M/L_K = 1.2$ which is the high end of the scale for the Kroupa initial mass function (IMF) of an old stellar population. The SNs have reached the TG limit by 30 kpc, so cannot contribute any more mass.

The problem is that NGC 720 has a relatively young stellar population, although there is an age gradient from ∼12 Gyr in the centre to ∼3 Gyr by ∼1 kpc (Humphrey et al. 2006). This leads to significant systematic uncertainty in constraining the M/L_K, which was given as 0.54 ± 0.11 and 0.35 ± 0.07 for the Salpeter and Kroupa IMF, respectively. A recent re-evaluation, with data of superior resolution (D. Buote, private communication), puts the Kroupa value at 0.49 ± 0.18 (meaning the Salpeter value will be somewhat larger), but this still falls short of the necessary galactic mass. This could be a serious problem if the low M/L_K could be confirmed, but for now it is a prediction of this model that the true M/L_K (when the correct IMF, age distribution and merger history are taken into account) will be close to 1.2.

NGC 720 is not the only system that is very sensitive to the observations. NGC 1550 was studied by Gastaldello et al. (2007) with both *Chandra* and *XMM–Newton* and both sets of temperature data are plotted in their Fig. 3. Later it was observed again by Kawaharada et al. (2009) using *XMM–Newton*, in a study which suggested there was evidence for a recent merger. If we use either set of *XMM–Newton* data points, the M/L_K would need to be at least 1.6, whereas if we only subscribe to the *Chandra* data, the M/L_K need only be 1.2. Follow-up observations could provide a very strong test of the model, but *Chandra*'s greater spatial resolution currently makes it the more reliable data set. A general point about these small groups of galaxies, where the brightest group galaxy is so dominant, is that the influence of triaxiality of the SN halo should eventually be investigated.

4.2 Sterile neutrino mass and the μ-function

Angus (2009) demonstrated that $11\,\mathrm{eV\,c^{-2}}$ SNs were required to fit the first three acoustic peaks of the CMB and that two species of $5.5\,\mathrm{eV\,c^{-2}}$ SNs were totally inadequate (as were three $2.2\,\mathrm{eV\,c^{-2}}$ ordinary neutrinos). There was also very little freedom to modify the mass by more than 5 per cent from $11\,\mathrm{eV\,c^{-2}}$, without introducing unjustified free parameters.

For further instruction to the importance of the SN mass to be $11\,\mathrm{eV\,c^{-2}}$, we calculated the M/L_K necessary to produce an equilibrium SN distribution in the group ESO-306 (which is by no means the most constraining) in two different scenarios. First, trying a $10.5\,\mathrm{eV\,c^{-2}}$ SN and secondly keeping an $11\,\mathrm{eV\,c^{-2}}$ SN mass but using the standard μ-function of MOND: where instead of using equation (4), we try $\mu(g/a_\mathrm{o}) = \frac{g/a_\mathrm{o}}{\sqrt{1+(g/a_\mathrm{o})^2}}$.

Whereas using the simple μ-function and an $11\,\mathrm{eV\,c^{-2}}$ SN requires $M/L_K = 1$, the $10.5\,\mathrm{eV\,c^{-2}}$ SN requires $M/L_K = 1.5$ and the standard μ-function would need 1.4. Given that these sorts of high M/L_K would be the rule, rather than the exception, they seem incompatible with stellar population synthesis models.

This evidence in favour of the simple μ-function is not an isolated case. In Famaey & Binney (2005) and McGaugh (2008), the simple function was preferred from a fit to the Milky Way's rotation curve (a high surface brightness galaxy) as was the case in the large sample of high surface brightness galaxies studied by Sanders & Noordermeer (2007). This preference is also being found by an ongoing study of ultra-high-resolution rotation curves observed by the H-I Near Galactic Survey (THINGS; Walter et al. 2005) collaboration (G. Gentile, private communication). The main problem with the simple function is that it cannot be used all the way to the strong gravity regime. In particular, it would produce too large a modification in the inner Solar system, which is excluded, for example, by measures of the perihelion precession of Mercury. The solution is to use a μ-function that would rapidly interpolate between the simple and standard μ for very large values of the gravitational acceleration, but this is not applicable here.

4.3 Common central phase-space density

It is an encouraging result that the $11\,\mathrm{eV\,c^{-2}}$ SNs have unique and continuous equilibrium models for such a large dynamic range of cluster properties, but what is remarkable is that at the centre of every cluster, the TG limit is reached. For each given cluster, there is a specific, maximum density profile that can exist in equilibrium – a good example being NGC 5129 (in Fig. 3), which must have the maximum allowed density from 40 kpc to the centre for the SN halo to both be in hydrostatic equilibrium and provide the correct dynamical mass as measured by the ICM properties.

Accordingly, it is the TG limit and the degenerate properties of the SNs (since they are fermions) that sets the dynamical properties of all clusters. No relation, even remotely, like this exists if the cluster DM is cold or non-fermionic.

4.4 Sterile neutrinos inside galaxies

4.4.1 Dynamics

It is apparent from the examples of NGC 4125 and NGC 6482 (see Section 4.1.7) that SNs will mostly not influence the dynamics of galaxies. Gentile et al. (2008) showed that a constant density of $10^{-5}\,\mathrm{M}_\odot\,\mathrm{pc}^{-3}$ was allowed in the MOND fits to the rotation curves of Ursa Major galaxies. This magnitude of SN density is typically found within 1 Mpc in the very massive clusters and within 100–300 kpc from the centre of groups. At the centres of clusters, the situation is obviously different, but stable spiral galaxies are never present there since tides would rip them apart before they fall to the centre. Therefore, this will not disturb the MOND Tully–Fisher relation since field spirals should be far from any SN haloes.

However, SNs are required to exist in the centres of some very massive ellipticals. This is clear from the right-hand panels of the enclosed mass profiles of the clusters A 478 (Fig. 1), A 907 and others. In these figures, one can see that the mass of the BCG (the solid line) is smaller than the MOND enclosed mass. Thus, a

considerable mass of SNs is required inside the limits of the stellar orbits, but always significantly less than the mass in stars.

4.4.2 Lensing studies of individual galaxies in MOND

In its original form, MOND should be able to explain all galaxy dynamics without DM. Although rotation curves have always yielded excellent results, the data for lensing studies (beginning with Zhao et al. 2006) of individual galaxies has not been as promising. For instance, Tian, Hoekstra & Zhao (2009) showed that the weak-lensing of single, isolated galaxies is perfectly compatible with MOND up to a particular galaxy luminosity (from $L_r = 0.1$–$8.0 \times 10^{10}\,\mathrm{L}_\odot$). Thereafter, the lensing data implies the need for DM, which is exactly as we might expect if these more luminous galaxies are embedded in a low density but extended SN halo (akin to those in the Humphrey et al. 2006 sample, see section 4.1.7).

The same is true for the study by Ferreras, Sakellariadou & Yusaf (2008) whereby the integrated mass along the line of sight is entangled with the stellar mass. This makes lensing studies of individual early-type galaxies in MOND significantly inferior to those using ICM, or even globular clusters (Richtler et al. 2008), planetary nebulae (Milgrom & Sanders 2003; Romanowsky et al. 2003; Douglas et al. 2007; Napolitano et al. 2009) and satellite galaxies (Angus et al. 2008b; Klypin & Prada 2009).

5 DISCUSSION AND CONCLUSION

In this paper, we have shown explicitly how to calculate the equilibrium configurations of neutrinos in MONDian galaxy clusters. The density of sterile neutrinos is fixed by the properties of the ICM (or the observed lensing map), but derivation of the sterile neutrino velocity dispersion allows a specific density profile to exist in hydrostatic equilibrium. We have presented the detailed properties of 30 typical galaxy groups and clusters over a wide range of masses and temperatures (and even redshift vis-a-vis the bullet cluster, the Lynx cluster and A 1689) and have shown that not only can we identify velocity dispersion profiles that allow the sterile neutrinos to exist in hydrostatic equilibrium, but also that the Tremaine–Gunn limit sets the central density.

It would appear to be a very strong coincidence that by doing little more than fixing the mass of a sterile neutrino to be $11\,\mathrm{eV\,c^{-2}}$, we can serendipitously, explain the formation of the acoustic peaks in the CMB and specify the *exact* properties of systems that require dark matter in MOND. In particular, regardless of cluster mass, the velocity dispersion of sterile neutrinos necessary to impose hydrostatic equilibrium allows the density to reach its maximum (which is a function of both sterile neutrino particle mass, velocity dispersion and cluster mass indirectly) at the centre of the cluster. The only stipulation is whether these equilibrium configurations are stable, which should be the next check.

Out of the 30 systems, there are two which need to be monitored. NGC 720 requires a K-band mass-to-light ratio of 1.2, which is possible for an old stellar population, but the current best population synthesis model suggests 0.49 ± 0.18. Estimates of stellar masses are notoriously fraught with difficulties (Conroy et al. 2009), but this is a potential problem. NGC 1550 (discussed alongside NGC 720 in Section 4.1.8) can only reproduce the X-ray temperature observed from *Chandra*; if the *XMM–Newton* data are used, the K-band mass-to-light ratio of the central galaxy is too high. From this study, it is clear that the strongest tests of the $11\,\mathrm{eV\,c^{-2}}$ sterile neutrino model come not from the rich clusters, but rather from smaller groups or individual galaxies with relatively bright X-ray haloes.

In a similar sense to how the NFW density profiles deduced from N-body simulations of CDM structure formation have been shown to be inadequate descriptions of some galaxy and galaxy cluster dark matter haloes (de Blok & McGaugh 1998; Gentile et al. 2004; Broadhurst & Barkana 2008), we suggest that our highly regular density and velocity dispersion profiles shown in Figs 1–6 must be used to judge the consistency of simulated structure growth in MOND cosmological simulations. Presumably, it is guaranteed that the objects that condense out of the background will reach the Tremaine–Gunn limit at the centre (which makes it so alluring that all the clusters studied here do), but it is not certain that the phase-space densities will fall with radius in the manner shown here, nor that the chemical potential will have the correct values.

Given that we fit the CMB and have these interesting results for clusters of galaxies, another crucial test of this model (after checking stability) will be to see if MOND N-body cosmological simulations, with $11\,\mathrm{eV\,c^{-2}}$ SNs can form structures resembling those shown here and match the matter power spectrum. It is worth pointing out that Skordis et al. (2006) computed the matter power spectrum with MOND-like gravity and three $2.75\,\mathrm{eV\,c^{-2}}$ active neutrinos (the a_o used was $3.5\times$ larger than the one used typically to fit rotation curves and used here) and showed the extra matter density from the neutrinos ($\Omega_\nu = 0.17$ compared to $\Omega_b = 0.05$) coupled with the MOND gravity could come relatively close to providing a good match to the matter power spectrum measured by the Sloan Digital Sky Survey (Tegmark et al. 2004). The higher matter density provided by our SNs ($\Omega_{\nu_\mathrm{s}} = 0.225$ and $\Omega_b = 0.047$) traded off with the smaller, more standard a_o, could very well provide a superior fit to the matter power spectrum. To resolve this, we need cosmological numerical simulations, which are still in their infancy (see Llinares, Knebe & Zhao 2008).

Finally, we remark that relativistic MOND theories beginning with TeVeS (Bekenstein 2004, also see the review by Skordis 2009) and BSTV (Sanders 2005), which led to new ideas like generalized Einstein–Aether (see e.g. Zlosnik, Ferreira & Starkman 2007, 2008), are still highly complex and only address the galactic dark matter problem (neither the cluster nor cosmological dark matter problem nor the dark energy problem). Therefore, one caveat we would add to our conclusions is that this cosmological model still requires dark energy in the same coincidental amount as Λ CDM. However, as elaborated upon in Milgrom (1999, 2009b), MOND and dark energy must be two sides of the same coin that leads seamlessly to $2\pi\, a_\mathrm{o} \approx c(\Lambda/3)^{1/2}$. There is some progress in this direction (Füzfa & Alimi 2007; Blanchet & Le Tiec 2009; Bruneton et al. 2009; Li & Zhao 2009) but it has not yet been convincingly or efficiently shown.

With respect to the prospect of a theoretical underpinning to the $11\,\mathrm{eV\,c^{-2}}$, something that is quite exciting is the use of non-commutative geometry models of gravity coupled to matter by Marcolli & Pierpaoli (2009) as a means to provide a natural explanation of issues like inflation and the origin of the small active neutrino masses. Three sterile neutrinos are expected in the theory – two massive ones ($>100\,\mathrm{GeV\,c^{-2}}$) facilitating the see-saw mechanism and a light one capable of being the dark matter. Whether a stable model exists where the light sterile neutrino is $11\,\mathrm{eV\,c^{-2}}$ has still to be investigated.

ACKNOWLEDGMENTS

GWA's research is supported by the University of Torino and Regione Piemonte. Partial support from the INFN grant PD51 is also gratefully acknowledged. BF acknowledges the financial

support of the Alexander von Humboldt foundation. We thank the referee for many insightful comments and both David A. Buote and Fabio Gastaldello for providing the ICM temperature and density data in electronic format.

REFERENCES

Abazajian K., Fuller G. M., Patel M., 2001, Phys. Rev. D, 64, 023501
Aguilar A., Auerbach L. B., Burman R. L., Caldwell D. O., Church E. D., Cochran A. K., Donahue J. B., Fazely A., 2001, Phys. Rev. D, 64, 112007
Aguirre A., Schaye J., Quataert E., 2001, ApJ, 561, 550
Angus G. W., 2008, MNRAS, 387, 1481
Angus G. W., 2009, MNRAS, 394, 527
Angus G. W., McGaugh S. S., 2008, MNRAS, 383, 417
Angus G. W., Shan H. Y., Zhao H. S., Famaey B., 2007, ApJ, 654, L13
Angus G. W., Famaey B., Buote D. A., 2008a, MNRAS, 387, 1470
Angus G. W., Famaey B., Tiret O., Combes F., Zhao H. S., 2008b, MNRAS, 383, L1
Bekenstein J. D., 2004, Phys. Rev. D, 70, 083509
Bekenstein J., 2006, Contemp. Phys., 47, 387
Bell E. F., de Jong R. S., 2001, ApJ, 550, 212
Blanchet L., Le Tiec A., 2009, Phys. Rev. D, 80, 023524
Bournaud F. et al., 2007, Sci, 316, 1166
Boyarsky A., Ruchayskiy O., Iakubovskyi D., 2009, J. Cosmol. Astropart. Phys., 3, 5
Bradač M. et al., 2006, ApJ, 652, 937
Broadhurst T. J., Barkana R., 2008, MNRAS, 390, 1647
Bruneton J.-P., Liberati S., Sindoni L., Famaey B., 2009, J. Cosmol. Astropart. Phys., 3, 21
Buote D. A., Canizares C. R., 1994, ApJ, 427, 86
Buote D. A., Canizares C. R., 1996, ApJ, 468, 184
Buote D. A., Jeltema T. E., Canizares C. R., Garmire G. P., 2002, ApJ, 577, 183
Clowe D., Gonzalez A., Markevitch M., 2004, ApJ, 604, 596
Clowe D., Bradač M., Gonzalez A. H., Markevitch M., Randall S. W., Jones C., Zaritsky D., 2006, ApJ, 648, L109
Conroy C., Gunn J. E., White M., 2009, ApJ, 699, 486
de Blok W. J. G., McGaugh S. S., 1998, ApJ, 508, 132
Donato F. et al., 2009, MNRAS, 397, 1169
Douglas N. G. et al., 2007, ApJ, 664, 257
Dunkley J. et al., 2009, ApJS, 180, 306
Famaey B., Binney J., 2005, MNRAS, 363, 603
Famaey B., Gentile G., Bruneton J.-P., Zhao H., 2007, Phys. Rev. D, 75, 063002
Feix M., Fedeli C., Bartelmann M., 2008, A&A, 480, 313
Ferreras I., Sakellariadou M., Yusaf M. F., 2008, Phys. Rev. Lett., 100, 031302
Füzfa A., Alimi J.-M., 2007, Phys. Rev. D, 75, 123007
Gastaldello F., Buote D. A., Humphrey P. J., Zappacosta L., Bullock J. S., Brighenti F., Mathews W. G., 2007, ApJ, 669, 158
Gavazzi R., Adami C., Durret F., Cuillandre J.-C., Ilbert O., Mazure A., Pelló R., Ulmer M. P., 2009, A&A, 498, L33
Gentile G., Salucci P., Klein U., Vergani D., Kalberla P., 2004, MNRAS, 351, 903
Gentile G., Famaey B., Combes F., Kroupa P., Zhao H. S., Tiret O., 2007, A&A, 472, L25
Gentile G., Zhao H. S., Famaey B., 2008, MNRAS, 385, L68
Gentile G., Famaey B., Zhao H., Salucci P., 2009, Nat, 461, 627
Giunti C., Laveder M., 2008, Phys. Rev. D, 77, 093002
Gnedin O. Y., Zhao H., 2002, MNRAS, 333, 299
Halkola A., Seitz S., Pannella M., 2006, MNRAS, 372, 1425
Hastings N. C., 2009, preprint (arXiv:0905.1211)
Hofmann S., Schwarz D. J., Stöcker H., 2001, Phys. Rev. D, 64, 083507
Humphrey P. J., Buote D. A., Gastaldello F., Zappacosta L., Bullock J. S., Brighenti F., Mathews W. G., 2006, ApJ, 646, 899
Jee M. J., White R. L., Ford H. C., Illingworth G. D., Blakeslee J. P., Holden B., Mei S., 2006, ApJ, 642, 720
Kawaharada M., Makishima K., Kitaguchi T., Okuyama S., Nakazawa K., Matsushita K., Fukazawa Y., 2009, ApJ, 691, 971
Khosroshahi H. G., Maughan B. J., Ponman T. J., Jones L. R., 2006, MNRAS, 369, 1211
Klypin A., Prada F., 2009, ApJ, 690, 1488
Klypin A., Kravtsov A. V., Valenzuela O., Prada F., 1999, ApJ, 522, 82
Kroupa P., Theis C., Boily C. M., 2005, A&A, 431, 517
Kubo J. M., Stebbins A., Annis J., Dell'Antonio I. P., Lin H., Khiabanian H., Frieman J. A., 2007, ApJ, 671, 1466
Kusenko A., 2009, preprint (arXiv:0906.2968)
Kuzio de Naray R., McGaugh S. S., Mihos J. C., 2009, ApJ, 692, 1321
Li B., Zhao H., 2009, Phys. Rev. D, 80, 064007
Lin Y.-T., Mohr J. J., 2004, ApJ, 617, 879
Lindner M., Ohlsson T., Seidl G., 2002, Phys. Rev. D, 65, 053014
Llinares C., Knebe A., Zhao H., 2008, MNRAS, 391, 1778
Mahdavi A., Finoguenov A., Böhringer H., Geller M. J., Henry J. P., 2005, ApJ, 622, 187
Maltoni M., Schwetz T., 2007, Phys. Rev. D, 76, 093005
Marcolli M., Pierpaoli E., 2009, preprint (arXiv:0908.3683)
Markevitch M., Gonzalez A. H., David L., Vikhlinin A., Murray S., Forman W., Jones C., Tucker W., 2002, ApJ, 567, L27
McGaugh S. S., 2005a, Phys. Rev. Lett., 95, 171302
McGaugh S. S., 2005b, ApJ, 632, 859
McGaugh S. S., 2008, ApJ, 683, 137
McGaugh S. S., de Blok W. J. G., 1998, ApJ, 499, 66
McGaugh S. S., Schombert J. M., Bothun G. D., de Blok W. J. G., 2000, ApJ, 533, L99
Milgrom M., 1983, ApJ, 270, 365
Milgrom M., 1995, ApJ, 455, 439
Milgrom M., 1999, Phys. Lett. A, 253, 273
Milgrom M., 2007, ApJ, 667, L45
Milgrom M., 2008a, New Astron. Rev., 51, 906
Milgrom M., 2008b, preprint (arXiv:0801.3133)
Milgrom M., 2009a, MNRAS, 398, 1023
Milgrom M., 2009b, ApJ, 698, 1630
Milgrom M., Sanders R. H., 2003, ApJ, 599, L25
Moore B., Ghigna S., Governato F., Lake G., Quinn T., Stadel J., Tozzi P., 1999, ApJ, 524, L19
Napolitano N. R. et al., 2009, MNRAS, 393, 329
Natarajan P., Zhao H., 2008, MNRAS, 389, 250
Navarro J. F., Frenk C. S., White S. D. M., 1997, ApJ, 490, 493
Neumann D. M., Lumb D. H., Pratt G. W., Briel U. G., 2003, A&A, 400, 811
Peacock J. A., 1999, Cosmological Physics. Cambridge Univ. Press, Cambridge
Pointecouteau E., Silk J., 2005, MNRAS, 364, 654
Randall S. W., Jones C., Markevitch M., Blanton E. L., Nulsen P. E. J., Forman W. R., 2009, ApJ, 700, 1404
Reichardt C. L. et al., 2009, ApJ, 694, 1200
Richtler T., Schuberth Y., Hilker M., Dirsch B., Bassino L., Romanowsky A. J., 2008, A&A, 478, L23
Romanowsky A. J., Douglas N. G., Arnaboldi M., Kuijken K., Merrifield M. R., Napolitano N. R., Capaccioli M., Freeman K. C., 2003, Sci, 301, 1696
Sánchez-Salcedo F. J., Hernandez X., 2007, ApJ, 667, 878
Sanders R. H., 1994, A&A, 284, L31
Sanders R. H., 1999, ApJ, 512, L23
Sanders R. H., 2003, MNRAS, 342, 901
Sanders R. H., 2005, MNRAS, 363, 459
Sanders R. H., 2007, MNRAS, 380, 331
Sanders R. H., McGaugh S. S., 2002, ARA&A, 40, 263
Sanders R. H., Noordermeer E., 2007, MNRAS, 379, 702
Serra A. L., Angus G. W., Diaferio A., 2009, preprint (arXiv:0907.3691)
Skordis C., 2009, Class. Quantum Gravity, 26, 143001
Skordis C., Mota D. F., Ferreira P. G., Bohm C., 2006, Phys. Rev. Lett., 96, 011301
Spergel D. N., Bean R., Doré O., Nolta M. R., Bennett C. L., Dunkley J., Hinshaw G., Wright E. L., 2007, ApJS, 170, 377

Tegmark M. et al., 2004, ApJ, 606, 702
The L. S., White S. D. M., 1988, AJ, 95, 1642
Tian L., Hoekstra H., Zhao H., 2009, MNRAS, 393, 885
Tremaine S., Gunn J. E., 1979, Phys. Rev. Lett., 42, 407 (TG)
Vikhlinin A., Kravtsov A., Forman W., Jones C., Markevitch M., Murray S. S., Van Speybroeck L., 2006, ApJ, 640, 691
Walter F., Brinks E., de Blok E., Bigiel F., Thornley M., Kennicutt R. C., 2005, Bull. Am. Astron. Soc., 37, 1258
Zappacosta L., Buote D. A., Gastaldello F., Humphrey P. J., Bullock J., Brighenti F., Mathews W., 2006, ApJ, 650, 777
Zhao H., Bacon D. J., Taylor A. N., Horne K., 2006, MNRAS, 368, 171
Zlosnik T. G., Ferreira P. G., Starkman G. D., 2007, Phys. Rev. D, 75, 044017
Zlosnik T. G., Ferreira P. G., Starkman G. D., 2008, Phys. Rev. D, 77, 084010

This paper has been typeset from a TEX/LATEX file prepared by the author.